A&A 404, L37–L41 (2003)
DOI: 10.1051/0004-6361:20030709

Astronomy & Astrophysics

Joint observations of propagating oscillations with SOHO/CDS and TRACE

M. S. Marsh[1], R. W. Walsh[1], I. De Moortel[2], and J. Ireland[3]

[1] Centre for Astrophysics, University of Central Lancashire, Preston, PR1 2HE, England
[2] School of Mathematics and Statistics, University of St. Andrews, North Haugh, St. Andrews, KY16 9SS, Scotland
[3] L3 Communications EER Systems Inc., NASA GSFC, Code 682.3, Bldg. 26, Greenbelt, MD 20771, USA

Received 18 March 2003 / Accepted 12 May 2003

Abstract. Joint Observing Program (JOP) 83 Solar and Heliospheric Observatory/Coronal Diagnostic Spectrometer (SOHO/CDS) and Transition Region and Coronal Explorer (TRACE) data is analysed for evidence of propagating intensity oscillations along loop structures in the solar corona. A propagating intensity oscillation with a minimum estimated speed of 50–195 km s^{-1} is observed within a TRACE 171 Å coronal loop using a running difference method. Co-spatial and co-temporal CDS and TRACE observations of this loop are analysed using a wavelet analysis method. The TRACE data shows a propagating oscillation with a period of ≈300 s. This period is also observed with CDS suggesting propagating oscillations at chromospheric, transition region and coronal temperatures in the He I, O V and Mg IX lines.

Key words. Sun: Corona – Sun: oscillations – Sun: Transition Region – Sun: UV radiation – waves

1. Introduction

The mechanism by which energy is transported and dissipated to heat the solar corona is an important and unresolved problem. The dissipation of Magneto-hydrodynamic (MHD) waves is a significant line of research in this area and observational quantification of these waves is needed to establish a realistic model of the energy balance in the outer solar atmosphere. Since the energy carried by MHD waves must ultimately originate from the solar convection zone, it is important to determine their properties as they propagate through the atmosphere.

Recent observations of oscillations in the corona are interpreted as fast/slow magneto-acoustic mode oscillations. DeForest & Gurman (1998) report on the observation of compressive wave trains in polar plumes; Ofman et al. (1999) suggest that these may be caused by the presence of magneto-acoustic waves. Recent results on observations that are interpreted as slow magneto-acoustic modes are described by Ireland et al. (1999), Banerjee et al. (2001), Hansteen et al. (2001), Robbrecht et al. (2001) and Marsh et al. (2002).

De Moortel et al. (2002a,b) give an overview of propagating intensity oscillations in coronal loops observed with the Transition Region and Coronal Explorer (TRACE, Handy et al. 1999). They find these oscillations in the footpoints of large diffuse coronal loops that are located close to active regions. These oscillations are interpreted as slow magneto-acoustic waves with propagation speeds in the range 70–235 km s^{-1} with periods of 282 ± 93 s that are damped very quickly along the loop (within 8.9 ± 4.4 Mm). De Moortel et al. (2002c) comment on the relation between 3 min oscillations found in TRACE coronal loops situated above sunspot regions and 5 min oscillations found in "non-sunspot" loops.

Brynildsen et al. (2002) and O'Shea et al. (2002) discuss the 3 min oscillations above sunspots using TRACE and the Coronal Diagnostic Spectrometer data (CDS, Harrison et al. 1995). They find that the oscillation amplitude above the umbra increases with temperature, reaches a maximum for lines formed close to 1–2 × 10^5 K and decreases at higher temperatures.

In this paper we discuss a 5 min oscillation in a "non-sunspot" coronal loop observed on 7th April 2000 using TRACE and CDS; part of the same data set used by De Moortel et al. (2002a). We present results which suggest that a propagating disturbance observed in TRACE at coronal temperatures is also present in co-spatial/co-temporal CDS-NIS (Normal Incidence Spectrometer) observations at chromospheric, transition region and coronal temperatures. Section 2 describes the observations while Sect. 3 describes the methods of preparation and analysis of the data. Section 4 presents the results obtained and interpretation and discussion is given in Sect. 5.

2. Observations

The observations are taken as part of the Joint Observing Program (JOP) 83 – "High Cadence Activity Studies and the Heating of Coronal Loops". The aim of this JOP was to investigate the rapid time variation in and around a target coronal

Send offprint requests to: M. S. Marsh,
e-mail: mmarsh@uclan.ac.uk

Article published by EDP Sciences and available at http://www.aanda.org or http://dx.doi.org/10.1051/0004-6361:20030709

loop system. The observations consist of co-temporal TRACE and CDS data with the position of the CDS slit located within the TRACE field of view. The TRACE observations analysed are 512″ × 512″ images taken in the 171 Å passband at 1″ resolution and run from 11:51–12:12 UT at a cadence of 9 s. The CDS data uses two observing sequences performed with NIS, LARGEBP2 and LOOPS_5. LARGEBP2 uses the 2″ × 240″ slit at 120 locations to produce a 240″ × 240″ context image in 16 spectral windows. LOOPS_5 uses the 2″ × 240″ slit at one location to take data in the following lines: He I 584 Å, O V 639 Å, WW 558.30 Å (wavelength band), and Mg IX 368 Å. These observations run from 11:54–12:24 UT at a cadence of 15 s.

3. Analysis

3.1. Preparation of the data

The CDS data must be cleaned and calibrated to correct a number of effects before the data can be analysed. The data is cleaned for cosmic ray spikes and corrected for detector bias and flat field. The CDS pointing is updated from an OPS calibration database. The rotation and tilt corrections are applied to the spectra and the mis-alignment between NIS-1 and NIS-2 is corrected. These corrections are applied using CDS_NEW_SPIKE, VDS_CALIB, UPD_CDS_POINT, NIS_ROTATE and relevant keywords. Since the loss of SOHO NIS-1 has shown a decrease in responsivity. We use a reasonable estimate for the correction factor of 1.8 for NIS-1 (Thompson 2003).

Standard corrections and preparations are applied to the TRACE data using TRACE_PREP and appropriate keywords. The pointings of the various bandpasses used by TRACE are offset from the white light values used in the TRACE index structure. This offset is of the order 2.15″ E 3.60″ N for the EUV channels and is corrected. The data is cleaned for cosmic ray spikes and streaks, the ADC offset and the background diffraction pattern are removed.

3.2. Pointing discrepancy and correlation of the data

When the LARGEBP2 image produced by CDS in a coronal temperature line such as Mg IX is compared to the TRACE images it is evident that there is a difference in the pointing between the two instruments. This is apparent in the different location of features visible in both images even when the pointings are corrected for rotation. Since we are trying to observe the sun at the same location with two different instruments simultaneously, it is important that we find a satisfactory method of relating the pointing.

To achieve this a 2-D cross correlation technique is used. The area in the TRACE image that corresponds to the position of the LARGEBP2 image is selected and normalised to have the same mean intensity as the LARGEBP2 image. A 2-D cross correlation method is then applied to determine the offset between the two images. In this data the first TRACE image is offset 10.2″ E and 3.6″ N relative to the CDS LARGEBP2 image after taking account of rotation. The pointings in the TRACE index structure are then corrected by these offset values and the

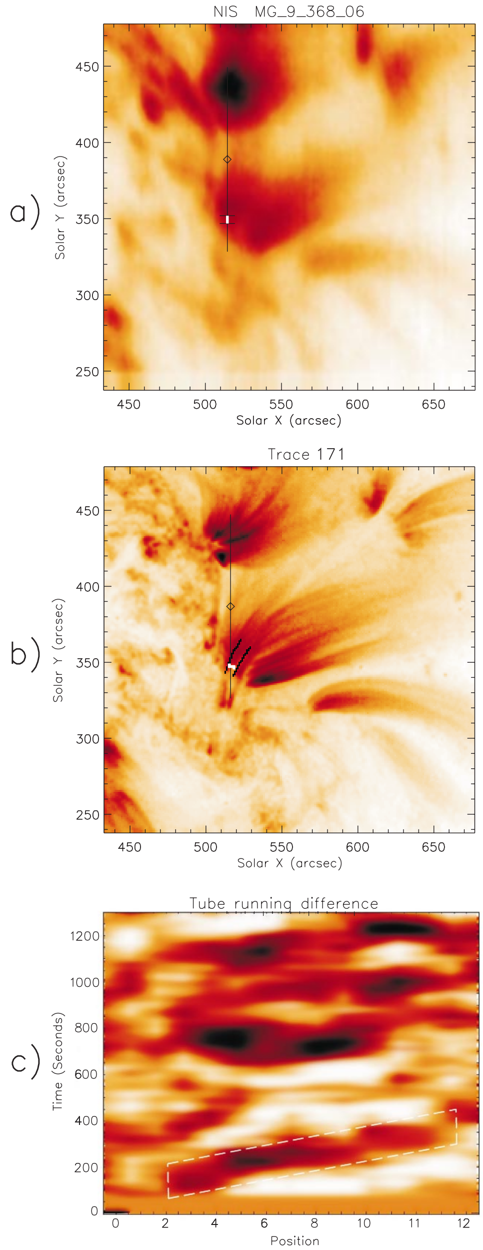

Fig. 1. a) NIS Mg IX context image indicating the position of the CDS slit (black line) and the pixels that form the CDS time series (white line); **b)** TRACE 171 context image with the CDS slit, tube (black arcs) defined for TRACE analysis and the cross section used to form the TRACE time series at position 4 along the tube (white band); **c)** running difference image formed from the tube in b). The dashed box outlines a dark band indicating propagation along the tube.

above process is repeated. A data cube is then extracted from the TRACE data that has the corrected coincident pointing with CDS, producing Figs. 1a,b. These are plotted with bilinear interpolation applied to increase image clarity.

3.3. Data analysis

The position of the LOOPS_5 slit can be seen in the context of the CDS LARGEBP2 Mg IX 368 Å and TRACE 171 Å observations (Figs. 1a,b). Considering the TRACE data, a tube is

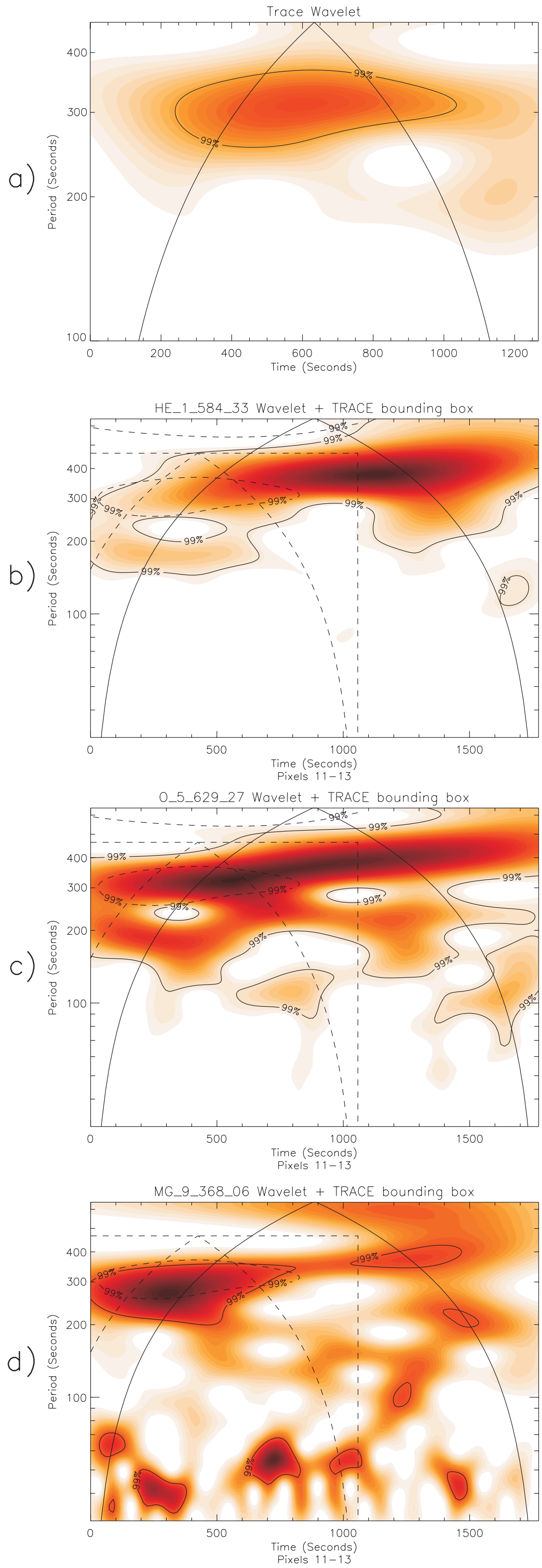

Fig. 2. Wavelet power spectra: **a)** for TRACE time series produced by the cross section indicated in Fig. 1b; **b)** for CDS He I time series from the pixels indicated in Fig. 1a with the position of the TRACE power spectrum (dashed lines) positioned relative to the timing of the CDS observations; **c)** as b) but indicating power for the CDS O V time series; **d)** as above but indicating power for the CDS Mg IX time series.

defined that overlies a coronal loop structure and the position of the CDS slit. Similar to De Moortel et al. (2002a) the length of the tube sides are normalised and cross sections are formed along the tube of 2″ width. The pixels are summed across a selected cross section to form a time series from the TRACE data. Figure 1b shows the defined tube as two black curves. The white band connecting these indicates the location of the selected tube cross section. This cross section is located close to the bottom of a coronal loop structure.

To form a time series from the LOOPS_5 data we sum 3 pixels (≈5″) along the CDS slit. Figure 1a indicates the selected pixels are coloured white and are bounded by two horizontal lines crossing the slit. These pixels overlie the position of the tube cross section used to form the TRACE time series.

To investigate any propagating intensity oscillations we use a running difference method as in De Moortel et al. (2002a). A running difference was formed by using the integrated intensity profile of the tube along its length and subtracting the profile of the tube 90 s earlier. Thus any propagating oscillation should appear as diagonal light and dark bands in the difference image.

The period of any oscillations within the TRACE and CDS time series are investigated using a wavelet analysis method. For a more detailed description of the wavelet analysis method see Marsh et al. (2002) and references within. The wavelet function and time series are finite, so the wavelet power spectrum suffers edge effects that are proportional to wavelet scale (wavelet scale is converted to equivalent Fourier period using a small correction factor). The cone shaped line in Fig. 2a for example is the cone of influence (COI) which marks the limit of these edge effects. The area beneath the COI and the x-axis can be considered free from these effects. The shaded regions in this figure indicate wavelet power of period p occurring at time t. To place an error estimate on the analysis, the wavelet power spectrum is compared to what would be expected from the appropriate noise distribution for each instrument. TRACE is assumed to have Poisson distributed noise and CDS is assumed to have Poisson distributed noise plus an instrumental contribution as described in Thompson (2000). A significance level is chosen representing the probability that the power can be considered as being real. We choose a significance level of 99% and any significant wavelet power is enclosed by a contour of significance.

4. Results

Figure 1a shows the LARGEBP2 context image in the Mg IX 368 Å line formed at a temperature of $\log T_e = 6.01$ while Fig. 1b shows the TRACE context image from the bandpass dominated by Fe IX 171 Å formed at $\log T_e = 5.99$. We can see the same coronal loop and moss structures with both instruments. The TRACE image shows clearly the context of the observations revealing the fine scale structure visible at 1″ × 1″ resolution compared to the 2.03″ × 1.68″ resolution of CDS. As described in Sect. 3.3 the location where the time series are extracted is indicated. We can see that this section is located at the base of a complex coronal loop configuration which is surrounded by moss.

The cross section of the tube chosen is approximately perpendicular to the filamentary structure of the loop and provides a good intersection with the CDS slit. This cross section is located at position 4 along the defined tube and can be located in the running difference image (Fig. 1c). The running difference image suggests that there is intensity propagation along the tube. This can be seen as a series of light and dark bands with a positive gradient. These bands appear to start before position 4 along the tube suggesting that the time series is located very close to the footpoint of the coronal loop, or at least very close to the origin where the oscillations are generated. Each position unit along the tube has a width of 2″ (≈1440 km). The band outlined by a dashed box in Fig. 1c was chosen as it represents the clearest example of a propagation. The gradient of this band gives a minimum estimate (due to projection effects) of the propagation speed. As an estimate of the uncertainty of the speed the gradient of the diagonals of the dashed box give maximum and minimum speeds in the range 50–195 km s^{-1}. This overlaps with the range of speeds reported in De Moortel et al. (2002a).

Figure 2a shows the wavelet power spectrum for the TRACE time series. The number of cycles within the COI is limited by the period of interest and the length of the time series. Due to edge effects we can only reliably comment on the period within the COI. The power spectrum shows a clear band of wavelet power above the confidence level, within the COI and centred around 300 s. The COI limits us to reliably observing ≈1.3 cycles. This could be increased by extending the duration of future similar observations.

It should be noted that Figs. 2b,c,d show the wavelet power spectra for the CDS time series and have the same start time. Figure 2a shows the TRACE power spectrum which begins 209 s before the CDS time series. Figure 2b shows the wavelet power spectrum for the CDS He I time series. The dashed lines plotted over this are taken from the TRACE wavelet power spectrum and indicate the boundaries of that spectrum , the COI and the significance contour of the ≈300 s period. We can see that He I has power at periods between ≈250–450 s and overlaps with the period found in TRACE. The centre of this band of power appears to have a slightly longer period in He I than in TRACE 171 Å. Figure 2c shows the wavelet power spectrum in O V. We see that there is a band of power present at periods between ≈200–500 s. The region of maximum wavelet power forms a band with ≈3 cycles present within the COI. The significant power in TRACE overlaps the power within the O V 99% confidence level very well. Figure 2c shows the wavelet power spectrum produced by Mg IX. We see power between ≈200–350 s but with only ≈1 cycle present within the CDS COI. Again the power overlaps well with that found in TRACE with the centre of this power appearing to have a slightly lower period in Mg IX than in TRACE 171 Å. The WW wavelength band was also analysed and power was found at a similar period. However, this power was only found at a confidence level of 95%.

The amplitude of the oscillations in He I, O V and Mg IX can be estimated using the deviation of the time series as a percentage of its mean intensity. We find amplitudes of 9.8 ± 3.1% for He I, 12.4 ± 2.1% for O V and 8.6 ± 1.2% for Mg IX. Brynildsen et al. (2002) present four observations above sunspot regions and find amplitudes ranging from 2.5–6% for He I, 7–16% for O V and 3–5% for Mg IX.

5. Conclusions

We find evidence of a propagating longitudinal intensity oscillation in a TRACE 171 Å coronal loop structure. A running difference method gives a minimum estimate of the propagation speed of 50–195 km s^{-1}. A wavelet analysis shows this to have a period of ≈300 s. The TRACE bandpass is dominated by emission from Fe IX 171 Å formed at $\log T_e = 5.99$. Wavelet analysis of co-spatial, co-temporal CDS-NIS data reveals a coincident period present in He I 584 Å ($\log T_e = 4.54$), O V 629 Å ($\log T_e = 5.4$) and Mg IX 368 Å ($\log T_e = 6.0$). The three CDS lines show a coincident period with the coronal TRACE data. O V formed at transition region temperatures appears to be better correlated with the TRACE 171 Å result than the He I (chromospheric) and Mg IX (coronal) lines.

The estimated amplitude of the oscillations in He I, O V and Mg IX are of the same order as those reported by Brynildsen et al. (2002). We also find that O V has the largest amplitude in agreement with their observation that the amplitude peaks in O V. However, also in sunspot regions O'Shea et al. (2002) found that the amplitude peaked in O III in the majority of cases.

As in De Moortel et al. (2002a) the propagating intensity oscillation observed in TRACE 171 Å is consistent with the interpretation of a slow magneto-acoustic wave. It should also be noted that Cooper et al. (2003) state that line of sight effects may allow kink modes to be observed as propagating disturbances in emission intensity. The results from the CDS data imply that this oscillation is also present at chromospheric, transition region and coronal temperatures. The observed period also coincides with the photospheric 5-min period. These combined factors suggest that there is a coupling and propagation of slow magneto-acoustic/kink waves at photospheric, chromospheric, transition region and coronal temperatures at the same location.

Let us consider the results from the TRACE analysis. Figure 1b shows the tube we have defined for the analysis, bounding the coronal loop structure that crosses the CDS slit. We see that the CDS slit also crosses loop structures towards the top of the slit. These loops do show some propagation in their TRACE running difference images. However, they are quickly damped and do not show any oscillation above the wavelet analysis confidence level at the position of the CDS slit. This indicates the need for accurate pointing to position the CDS slit close to the loop footpoints.

Three days of JOP 83 data were analysed on the 7th, 8th and 9th of April 2000 during this work. The CDS and TRACE data were analysed at 70 positions overlying the CDS slit over this period. The example presented here represents the best example of a coincident period within CDS and TRACE. The paucity of examples is likely due to undesirable pointing of the CDS with respect to the coronal loop structures combined with mistimed observations.

Acknowledgements. M.S. Marsh is supported by a PPARC research studentship. R.W. Walsh is supported by a Leverhulme Trust Research Fellowship. Data provided courtesy of TRACE and SOHO/CDS consortium. SOHO is a project of international co-operation between ESA and NASA. Wavelet software was provided by C. Torrence and G. Compo, and is available at URL: `http://paos.colorado.edu/research/wavelets`.

References

Banerjee, D., O'Shea, E., Doyle, J. G., & Goossens M. 2001, A&A, 371, 1137
Brynildsen, N., Maltby, P., Fredvik, T., & Kjeldseth-Moe, O. 2002, Sol. Phys., 207, 259
Cooper, F. C., Nakariakov, V. M., & Tsiklauri, D. 2003, A&A, 397, 765
Deforest, C. E. & Gurman, J. B. 1998, AJ, 501, L217
De Moortel, I., Ireland, J., Walsh, R. W., & Hood, A. W. 2002a, Sol. Phys., 209, 61
De Moortel, I., Ireland, J., Walsh, R. W., & Hood, A. W. 2002b, Sol. Phys., 209, 89
De Moortel, I., Ireland, J., Hood, A. W., & Walsh, R. W. 2002c, A&A, 387, L13
Handy, B. N., Acton, L. W., Kankelborg, C. C., et al. 1999, Sol. Phys., 187, 229
Hansteen, V. H., Betta, R., & Carlsson, M. 2001, A&A, 360, 742
Harrison, R. A., Sawyer, E. C., Carter, M. K., et al. 1995, Sol. Phys., 163, 233
Ireland, J., Walsh, R. W., Harrison, R. A., & Priest, E. R. 1999, A&A, 347, 355
Marsh, M. S., Walsh, R. W., & Bromage, B. J. I. 2002, A&A, 393, 649
Ofman, L., Nakariakov, V. M. & Deforest, C. E. 1999, AJ, 514, 441
O'Shea, E., Muglach, K., & Fleck, B. 2002, A&A, 387, 642
Robbrecht, E., Verwichte, E., Berghmans, D., et al. 2001, A&A, 370, 591
Thompson, W. T. 2000, CDS Software Note No. 49
Thompson, W. T. 2003, Personal communication